

Available online at www.sciencedirect.com

ScienceDirect

Biomedical Journal

journal homepage: www.elsevier.com/locate/bj

Original Article

Doxycycline hyclate stimulates inducible nitric oxide synthase and arginase imbalance, potentiating inflammatory and oxidative lung damage in schistosomiasis

Matheus Augusto Souza ^a, Elda Gonçalves-Santos ^a,
Reggiani V. Gonçalves ^c, Eliziária C. Santos ^d, Camila C. Campos ^a,
Marcos J. Marques ^b, Raquel L.M. Souza ^b, Rômulo D. Novaes ^{a,*}

^a Institute of Biomedical Sciences, Department of Structural Biology, Federal University of Alfenas, Alfenas, Minas Gerais, Brazil

^b Institute of Biomedical Sciences, Department of Pathology and Parasitology, Federal University of Alfenas, Alfenas, Minas Gerais, Brazil

^c Department of Animal Biology, Federal University of Viçosa, Viçosa, Minas Gerais, Brazil

^d School of Medicine, Federal University of Jequitinhonha and Mucuri Valleys, Diamantina, Minas Gerais, Brazil

ARTICLE INFO

Article history:

Received 26 April 2021

Accepted 21 December 2021

Available online 28 December 2021

Keywords:

Experimental pathology

Lung infection

Oxidative stress

Parasitology

Schistosomiasis

ABSTRACT

Background: We investigated the relationship between inducible nitric oxide synthase (iNOS) and arginase pathways, cytokines, macrophages, oxidative damage and lung granulomatous inflammation in *S. mansoni*-infected and doxycycline-treated mice.

Methods: Swiss mice were randomized in four groups: (i) uninfected, (ii) infected with *S. mansoni*, (iii) infected + 200 mg/kg praziquantel (Pzt), (iv) and (v) infected + 5 and 50 mg/kg doxycycline. Pzt (reference drug) was administered in a single dose and doxycycline for 60 days.

Results: *S. mansoni*-infection determined extensive lung inflammation, marked recruitment of M2 macrophages, cytokines (IL-4, IL-5, IFN- γ , TNF- α) upregulation, intense eosinophil peroxidase (EPO) levels, arginase expression and activity, reduced iNOS expression and nitric oxide (NO) production. The higher dose of doxycycline aggravated lung granulomatous inflammation, downregulating IL-4 levels and M2 macrophages recruitment, and upregulating iNOS expression, EPO, NO, IFN- γ , TNF- α , M1 macrophages, protein carbonyl and malondialdehyde tissue levels. The number and size of granulomas in doxycycline-treated animals was higher than untreated and Pzt-treated mice. Exudative/productive granulomas were predominant in untreated and doxycycline-treated animals, while fibrotic/involutive granulomas were more frequent in Pzt-treated mice. The reference treatment with Pzt attenuated all these parameters.

* Corresponding author. Institute of Biomedical Sciences, Federal University of Alfenas, Rua Gabriel Monteiro da Silva, 700, Alfenas, 37130-000, Minas Gerais, Brazil. Tel.: +55 31 3299 1300.

E-mail address: romulo.novaes@unifal-mg.edu.br (R.D. Novaes).

Peer review under responsibility of Chang Gung University.

<https://doi.org/10.1016/j.bj.2021.12.007>

2319-4170/© 2021 Chang Gung University. Publishing services by Elsevier B.V. This is an open access article under the CC BY-NC-ND license (<http://creativecommons.org/licenses/by-nc-nd/4.0/>).

Conclusion: Our findings indicated that doxycycline aggravated lung granulomatous inflammation in a dose-dependent way. Although Th1 effectors are protective against several intracellular pathogens, effective schistosomicidal responses are dependent of the Th2 phenotype. Thus, doxycycline contributes to the worsening of lung granulomatous inflammation by potentiating eosinophils influx and downregulating Th2 effectors, reinforcing lipid and protein oxidative damage in chronic *S. mansoni* infection.

At a glance commentary

Scientific background on the subject

Drugs of the tetracycline family, including doxycycline (Dox), exhibits toxic effects on *Schistosoma mansoni* worms *in vitro*. However, Dox exerts negative effects *in vivo*, aggravating liver inflammation in animals with schistosomiasis *mansoni*. Currently, it remains unclear whether this response is associated to Th1/Th2 imbalance and macrophages polarization.

What this study adds to the field

This study indicates for the first time that Dox aggravates lung granulomatous inflammation by upregulating Th1 cytokines, M1 macrophages accumulation, iNOS gene expression and NO production in detriment of arginase gene expression and activity. This study provides evidence that Dox acts as a pharmacological risk factor in schistosomiasis *mansoni*.

Schistosomiasis *mansoni* is a neglected tropical helminth infection caused by the trematode worm *Schistosoma mansoni*. This disease is endemic and responsible by high morbidity and mortality rates in developing countries, especially in South and Central America, Africa, and Middle East [1,2]. In these countries, schistosomiasis is more prevalent in poor rural communities, where hygiene habits, sanitation, and access to health services are deficient [3]. In these areas, the high frequency of gastropod snails (genus *Biomphalaria* - intermediate host) infected by *S. mansoni* in freshwater sources used by humans (definitive host) favors parasite life cycle and schistosomiasis spread [1,4,5].

After penetrating the skin of the definitive host, the parasites migrate to the heart and lungs via blood and lymphatic circulation [1,5,6]. Then, *S. mansoni* reaches the liver and mesenteric portal vessels, where they evolve into adult forms and start oviposition. Finally, the parasite eggs spread through the bloodstream and are trapped in multiple tissues and organs, triggering a systemic inflammation [6,7]. From venous portocaval shunts, *S. mansoni* eggs reach the lung parenchyma [7], and its soluble antigens trigger a marked granulomatous inflammation [2]. This process is dependent on a well-polarized Th2 phenotype, which orchestrates granuloma organization in a protective mechanism to isolate *S. mansoni* eggs, restrict

continuous antigenic stimulation and immunomediated tissue damage [8]. Conversely, the Th1 immune phenotype impairs granuloma organization, reinforcing continuous immunological activation, excessive inflammatory and prooxidant responses, which increases the susceptibility of *S. mansoni*-infected hosts to tissue damage and death [6,9].

In schistosomiasis *mansoni*, macrophages are intensively recruited to the parasitized organs and are alternatively activated by Th2 effectors (i.e., IL-4, IL-6 and IL-13). These alternatively activated macrophages (M2) express high arginase activity, are essential for structuring granulomas and are considered anti-inflammatory cells by antagonizing Th1 immunity and limiting tissue damage [9]. However, macrophages classically activated (M1) by Th1 effectors (i.e., IL-12, IFN- γ and TNF- α) show marked inducible nitric oxide synthase (iNOS) expression and intense nitric oxide (NO) production [4,8]. These cells are undesirable in Th2 protective immunological responses, presenting a central relevance in the defense against intracellular pathogens, although they are associated with an intense biosynthesis of prooxidant metabolites (i.e., O₂ \bullet^- , OH \bullet , and H₂O₂) [10] and extensive damage to the surrounding tissue [4,8]. In this sense, IL-4 production and M2 macrophages polarization are essential to increase host resistance to *S. mansoni* infection. Accordingly, stimuli that reinforce Th1/Th2 imbalance (i.e., co-infections, anti-parasitic and immunomodulatory drugs) can modify the pathophysiology of schistosomiasis, with a direct impact on organ damage and host mortality [4,8,11].

Drugs of the tetracycline family, including doxycycline (Dox), showed potent toxic effects and/or immunomodulatory properties in parasitic diseases caused by *Plasmodium falciparum* [12], *Trypanosoma cruzi* [13] different filarial species [14] and *S. mansoni* [12,15]. Previous evidence indicated that although Dox has a dose-dependent toxic effect on *S. mansoni in vitro* [2], this drug is potentially harmful *in vivo* [15]. Accordingly, Dox increased host susceptibility to *S. mansoni* infection by aggravates liver and lung inflammation, an effect potentially associated to the upregulation of leucocytes recruitment and the formation of more numerous large granulomas in mice [2,15]. However, it remains unclear whether this response to Dox treatment can be attributed to a subversion of the balance between Th1/Th2 molecules (i.e., cytokines, arginase, iNOS and NO) and M2 macrophages polarization in schistosomal granulomatous inflammation. Thus, the relationship between the expression and production of Th1/Th2 effectors, macrophages recruitment and phenotype with the severity of lung granulomatous inflammation in *S. mansoni*-infected and Dox-treated animals was investigated.

Materials and methods

Models of schistosomiasis and experimental groups

Swiss mice were randomized into four groups with 9 animals per group as follows: (Cnt) control uninfected untreated, (Sh) infected with *S. mansoni*, (ShP) infected with *S. mansoni* + praziquantel (Pzt, 200 mg/kg), (ShD1) infected with *S. mansoni* + Dox (5 mg/kg), and (ShD2) infected with *S. mansoni* + Dox (50 mg/kg). *S. mansoni* infection established from a subcutaneous injection of 25 cercariae of the LE strain [16,17]. *S. mansoni* infection was microscopically confirmed 80 days after inoculation by observation of parasite eggs in the feces [2]. Once the infection was confirmed, the animals were treated with the reference schistosomicidal drug Pzt [18] or with Dox. The animals received Dox daily by gavage for 60 days. Dox was administered at 5 and 50 mg/kg, corresponding to 10% and 100% of the reference dose associated to immunomodulatory effects in a murine model of *S. mansoni* infection [2]. Based on this model, 80 days of infection were objectively planned to ensure that the animals reached the chronic phase of schistosomiasis [17]. The experimental protocol was developed in animal facility with controlled humidity (45–65%), temperature (21 ± 2 °C) and photoperiod (12h–12h, light–dark cycles). The animals had free access to water and food [19].

Euthanasia, tissue collection and ethics

All animals were intraperitoneally anesthetized with ketamine (100 mg/kg) and xylazine (10 mg/kg) 24 h after the last treatment with Dx [2]. The lungs were collected and weighed. The relative lung mass was determined by dividing the lungs mass by the body mass. Cytokine levels, arginase and inducible nitric oxide synthase (iNOS) gene expression, NO levels, and arginase activities were quantified in 150 mg lung fragments. The remaining samples were used to analyze lipid, protein and DNA oxidation, and were preserved in fresh histological fixative (18h in 10% formalin, pH = 7.2, 0.1M) for microstructural analysis [20]. The institutional Ethics Committee for Animal Care approved this study (protocol 26/2018).

Lung histological processing

Lung fragments were fixed attached to a paraffin-coated Petri dish to minimize retraction. The samples were dehydrated ethyl alcohol, clarified in xylene and included in Paraplast tissue embedding medium (Sigma–Aldrich, San Luis, Missouri, USA). Semi-serial histological sections with 5- μ m thickness were obtained using a rotary microtome (Leica Biosystems, Wetzlar, Germany) [21]. The analysis of different lung areas was ensured by using one to each 50 sections. Histological sections were stained with hematoxylin and eosin (H&E) for histopathological [22,23] and morphometric [20] analyses. Lung sections were observed from a bright field photomicroscope (Axioscope A1, Carl Zeiss, Oberkochen, Germany), and 12 random digital lung images were obtained for each animal and

staining method using an image analysis software (Axion Vision LE, Carl Zeiss, Oberkochen, Germany) [16].

Lung histopathology and morphometry

Qualitative histopathological analysis was based on the identification of microstructural abnormalities such as hyperinflation or alveolar collapse, vascular congestion, hemorrhagic foci, thickening of the alveolar septum, inflammatory infiltrate [20,22], retention of *S. mansoni* eggs in the lung parenchyma, and distribution of schistosomal granulomas [2,11]. Histopathological results were determined from 12 histological fields randomly sampled for each animal using $\times 40$ objective lens ($\times 400$ magnification). Thus, $23.2 \times 10^5 \mu\text{m}^2$ total lung area was analyzed in each group. Lung microstructure of uninfected control animals was adopted as the morphological reference to estimate *S. mansoni*-induced lung abnormalities in infected animals.

Vertical lung sections were obtained to reduce measure bias in morphometric analysis [24,25]. The number of granulomas (NG) per lung area (n/mm^2) was estimated as follows: $\text{NG} (\text{n/mm}^2) = \Sigma_G / \text{At}$; where Σ_G corresponds to the number of granulomas observed in the microscopic fields and At is the dimension of the test area (here = $34 \times 10^3 \mu\text{m}^2$). From all granulomas analyzed, the relative distribution (%) of involutive (small, with low cellularity and intense collagens accumulation in the sheath) and productive granulomas (with high cellularity in the sheath and scarce collagen accumulation) was determined as previously reported [11]. These parameters were quantified in 12 microscopic lung areas randomly sampled for each animal using $\times 5$ objective lens ($\times 50$ magnification). Thus, $29.9 \times 10^7 \mu\text{m}^2$ total lung area was analyzed in each group. The size of lung granulomas was analyzed from classical morphometric techniques. Only granulomas showing well-defined *S. mansoni* eggs (centrally sectioned) were evaluated. Granuloma volume (V) was estimated using the prolate spheroid (PS) principle as follows: $V_{\text{PS}} = (4/3) \times \pi a^2 b$; where a is the smaller radius and b is the larger radius of a cross-sectioned ovoid structure [26]. These parameters were calculated from 180 granulomas per infected group, corresponding to 20 granulomas per animal [11]. All quantitative measures were operationalized from the Image-Pro Plus 4.5 software (Media Cybernetics Inc., Silver Spring, MD, USA) [17].

Eosinophil peroxidase assay

The eosinophil peroxidase enzyme (EPO) was used as a biochemical marker of tissue infiltration by eosinophils [27]. This enzyme was quantified in lung homogenate using a commercial colorimetric enzyme-linked immunosorbent assay (ELISA) kit, following the manufacturer's instructions (CUSABIO, Houston, TX, USA). The optical density of all reactions were obtained at 450 nm using a microplate reader (Anthos Zenyth 200, Biochrom, Cambridge, UK). This assay presented a detection range of 0.156–10 ng/mL. To avoid possible interferences related to variations in protein

extraction, the results were normalized to ng/mg protein. Thus, protein levels in the homogenates were quantified by the Bradford method [28].

Analysis of cytokines by cytometry bead array

Lung samples were homogenized in protease inhibitor cocktail (Sigma–Aldrich, San Luis, MO, USA) prepared in sodium phosphate buffer (pH = 7.2), centrifuged at 4 °C for 15 min (3800×g), and the supernatant collected. The cytokines interleukin-4 (IL-4), interleukin-5 (IL-5), interleukin-10 (IL-10), transforming growth factor β (TGF-β), interferon gamma (IFN-γ), and tumor necrosis factor-α (TNF-α) were quantified in the supernatant. All cytokines were quantified by flow cytometry bead array (CBA). Commercial kits were used following the manufacturer's instructions (BD Biosciences, San Diego, CA, USA). Cytokine levels were analyzed in the FACSVerse flow cytometer (BD Biosciences, San Diego, CA, USA). The results were obtained from the FCAP 3.0 software. Standard curves were prepared using recombinant cytokines at 20–5000 pg/mL. The lower limit of CBA-based cytokine detection was 2.5–52.7 pg/mL [2,29].

Arginase-1 and inducible nitric oxide synthase (iNOS) gene expression

Gene expression for arginase and inducible nitric oxide synthase (iNOS) was determined by quantitative real-time polymerase chain reaction (qPCR) as previously reported [11,30]. Briefly, mRNA was transcribed into cDNA from a reverse transcription commercial kit (ThermoFisher Scientific Waltham, MA, USA) following the manufacturer's instructions. All primers were commercially obtained from ThermoFisher Scientific (Waltham, MA, USA), and are indicated in Table 1. PCR reactions were developed using SYBR Green PCR Mastermix and the manufacturer's instructions (Applied Biosystems, Carlsbad, CA, USA). Gene expression was standardized to GAPDH expression.

Arginase activity and nitric oxide assay

Arginine activity was analyzed in lung homogenates as previously described [11]. Briefly, 1 mL of 10 mM MnCl₂ was incorporated to homogenate and the arginase was activated by heating the mixture for 10 min at 56 °C. Arginine hydrolysis was obtained by add 10 ml L-arginine (0.05 M) in lung

homogenate for 15–120 min at 37 °C (pH = 9.7). The reaction was blocked with a solution containing H₂SO₄ (96%) and H₃PO₄ (85%) prepared in distilled water (1/3/7, v/v/v). The urea concentration obtained from arginine hydrolysis was read in spectrophotometer at 540 nm after treatment with 4 mL α-isonitrosopropionone and for 30 min at 95 °C. One unity of arginase activity corresponded to 1 mM urea formation per min [30].

Nitric oxide levels were estimated by measuring nitrite/nitrate levels in lung homogenates from the Griess reaction as previously reported [31]. Briefly, lung homogenates were incubated with Griess reagent (1% sulfanilamide, 0.1% naphthalene diamine dihydrochloride, and 2.5% phosphoric acid, 1:1 v/v) at room temperature for 10 min. The reaction for NO was analyzed in spectrophotometer at 550 nm wavelength using a microplate reader (Anthos Zenyth 200, Biochrom, Cambridge, UK) [11].

Lipid, protein and DNA oxidation analysis

For analysis of lipid peroxidation, malondialdehyde (MDA) was quantified in lung samples. Briefly, lung tissue was homogenized in sodium phosphate buffer (0.1M, pH 7.2) and centrifuged for 10 min (10,000×g and 4 °C). The homogenate was treated with thiobarbituric acid solution (15% trichloroacetic acid, 0.25 N HCl, and 0.375% thiobarbituric acid) for 15 min. Then, malondialdehyde lung levels were measured by spectrophotometry (Anthos Zenyth 200; Biochrom, Cambridge, UK) at 535 nm using 96-wells polystyrene plates, as previously reported [32].

Protein oxidation was estimated considering the lung content of protein carbonyl (PCN) [23,32]. Briefly, PCN levels were quantified after incubating the lung pellets obtained from the MDA assay with 0.5 mL of 10 mM dinitrophenylhydrazine (DNPH). This assay is based on a reaction involving derivatization of the carbonyl group with 2,4-dinitrophenylhydrazine (DNPH), resulting in the production of 2,4-dinitrophenyl hydrazine (DNP), a stable product with red to orange color. After the reaction stabilized, the optical density was monitored by spectrophotometry at 370 nm [33].

For the DNA oxidation assay, nucleic acid was extracted from lung samples using proteinase K, phenol and chloroform, and 8-hydroxy-2'-deoxyguanosine (8-OHdG) levels were determined as reported [32]. Briefly, purified DNA was resuspended in 0.1 mmol/L EDTA and 10 mmol/L Tris–HCl, treated with 5 μg nuclease P1 (Aldrich Chemical Co., Milwaukee, USA) and 45 μl DNA samples. After DNA digestion (37 °C for 1 h), the samples were treated with 10 mmol/L MgCl₂, 500 mmol/L Tris–HCl, and 0.6 UI alkaline phosphatase (Aldrich Chemical Co., Milwaukee, USA) at 37 °C for 1 h. Then 8-OHdG levels were measured from enzyme linked immunosorbent assay (ELISA), following the manufacturer instructions (Cell Biolabs Inc., San Diego, CA, USA) [32].

Immunohistochemistry and image segmentation

Dewaxed lung sections were submitted to antigen retrieval with citrate buffer (pH 6.0) in a pressure cooker during 4 min [25]. The sections were then incubated with 3% H₂O₂ solution

Table 1 Primers used in quantitative polymerase chain reaction^a.

iNOS	Forward	5'-TTTGCTTCCATGCTAATGCGAAAG-3'
	Reverse	5'-GCTCTGTTGAGGTCTAAAGGCTCCG-3'
Arginase-1	Forward	5'-GGAAGCATCTTGGCCAGCC-3'
	Reverse	5'-TCCCAGAGCTGTTGTCAGGGG-3'
GAPDH	Forward	5'-ACTCCACTCAGGGCAAATTC-3'
	Reverse	5'-TCTCCATGGTGGTGAAGA CA-3'

Abbreviations: iNOS: inducible nitric oxide synthase, GAPDH: Glyceraldehyde 3-phosphate dehydrogenase.

^a All primers were validated and reported in a previous study: Free Radic Biol Med 2018; 129:227–236.

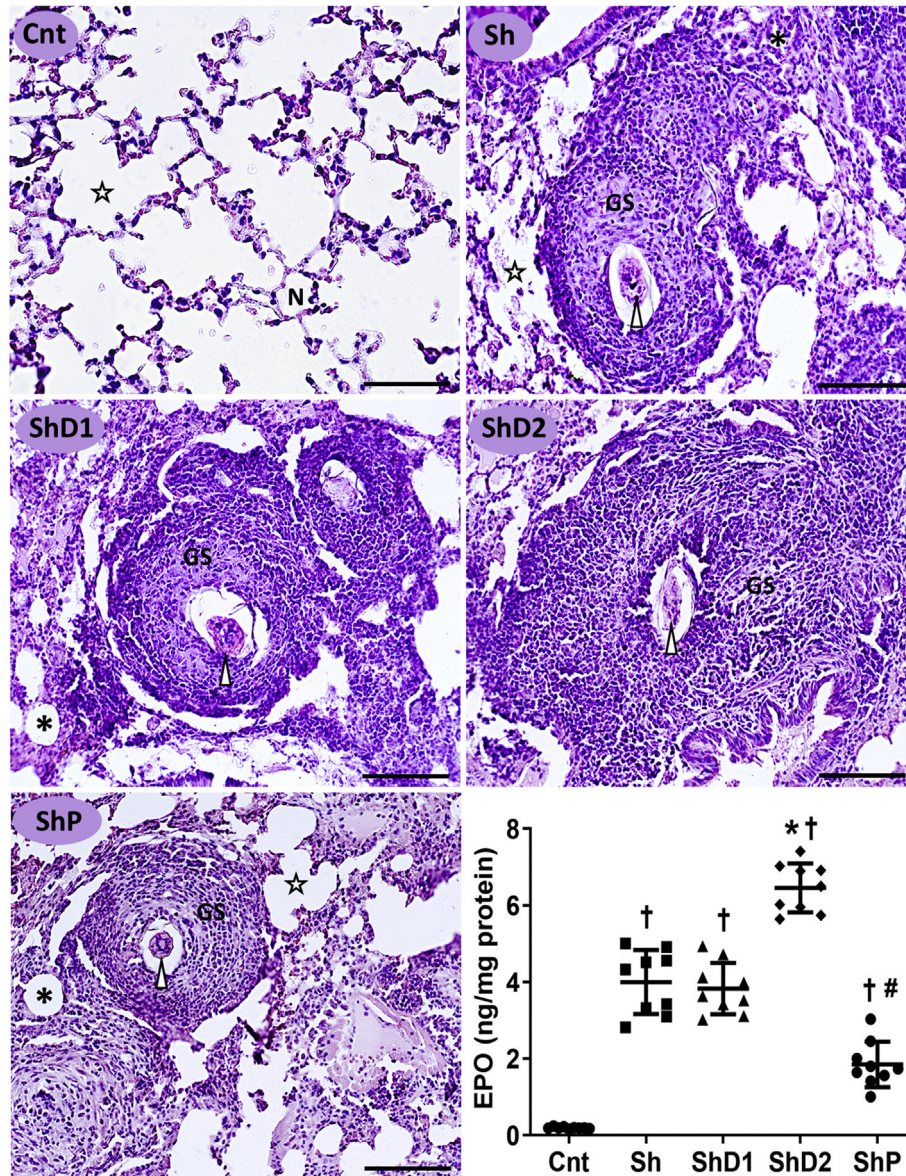


Fig. 1 Representative photomicrographs of the lungs and eosinophil peroxidase (EPO) levels (graphic) in the lung tissue from control uninfected and *Schistosoma mansoni*-infected mice untreated and treated with doxycycline hyclate (Bright field microscopy, hematoxylin and eosin staining, scale bar = 60 μ m). Groups: Cnt: control uninfected untreated, Sh: infected with *S. mansoni*, ShD1: infected treated with doxycycline hyclate (5 mg/kg), ShD2: infected treated with doxycycline hyclate (50 mg/kg), ShP: infected treated with praziquantel (Pzt, 200 mg/kg). Symbols in the microscopic images: Star = alveolar sac, N = normal alveoli, GS = granuloma sheath, asterisk = collapsed alveoli, arrowhead = *S. mansoni* egg. In the graphic, data are expressed as mean and standard deviation. The points denote EPO levels obtained for each animal in all groups. The symbols in each group indicate statistical difference ($p \leq 0.05$), compared to † Cnt, * Sh and ShD1, # Sh, ShD1 and ShD2.

for 10 min to block endogenous peroxidase and treated with 5% non-fat milk in TBST (0.05% Tween 20X with Tris-buffered saline, pH 7.6) by 15 min. Then, sections were incubated for 12h at 4 °C with a primary rabbit anti-iNOS antibody (1:1000 dilution) (PA3-030A, ThermoFisher Scientific, Waltham, MA, USA) for M1 macrophages [34] and anti-Arginase-1 (1:500 dilution) (PA5-29645, ThermoFisher Scientific, Waltham, MA, USA) for M2 macrophages [35]. Control slides were produced by omitting the primary antibody. The sections were then

incubated for 2h with a ready-to-use secondary goat anti-rabbit IgG antibody conjugated with horseradish peroxidase (Dako EnVision™+ Dual Link System-HRP, Agilent, Santa Clara, CA, USA). The slides were treated with TBST and the immunohistochemical reaction was revealed with 0.5% 3,3'-diaminobenzidine (DAB) during 5 min [25]. Finally, lung sections were dehydrated with ethyl alcohol, treated with xylene and mounted with Entellan (Merk, Darmstadt, Germany). Relative lung area occupied by M1 macrophages (iNOS

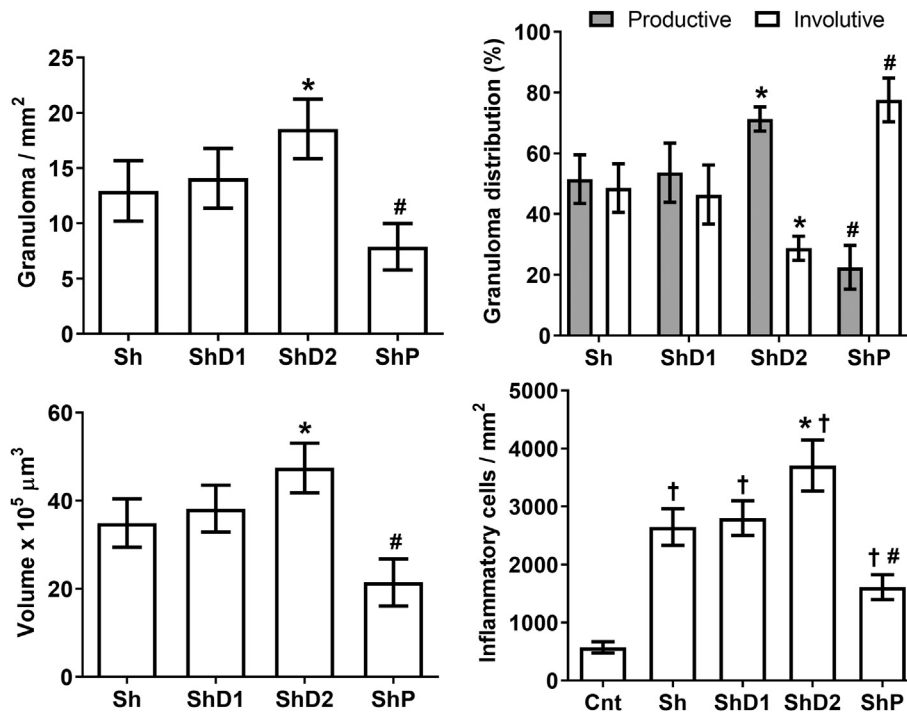


Fig. 2 Granuloma number and volume, distribution of granulomas according the evolutionary stages, and number of inflammatory cells in the lungs of control uninfected and *Schistosoma mansoni*-infected mice untreated and treated with doxycycline hyclate. Groups: Cnt: control uninfected untreated, Sh: infected with *S. mansoni*, ShD1: infected treated with doxycycline hyclate (5 mg/kg), ShD2: infected treated with doxycycline hyclate (50 mg/kg), ShP: infected treated with praziquantel (Pzt, 200 mg/kg). Data are expressed as mean and standard deviation. The symbols in each group indicate statistical difference ($p \leq 0.05$), compared to * Sh and ShD1, # Sh, ShD1 and ShD2, † Cnt.

marking) was estimated from a two-dimension color segmentation computational method [36], which was operationalized from color deconvolution and threshold toll of the ImageJ software as previously described [24]. Results were obtained from 12 microscopic images randomly sampled for each animal using $\times 40$ objective lens ($\times 400$ magnification).

Statistical analysis

The results were represented using mean and standard deviation (mean \pm S.D.) or median and interquartile range. Data distribution was evaluated using the Kolmogorov–Smirnov normality test. One-way ANOVA test was used to analyzed the variance of parametric data. Data with normal distribution were compared from the Student-Newman-Keuls test. Non-parametric data were compared by using the Kruskal–Wallis One-way ANOVA on Ranks test, followed by the Student-Newman-Keuls method for multiple comparisons. Correlations were investigated from linear regression analysis. All tests were based on 95% confidence, and results with p value ≤ 0.05 were statistically significant.

Results

As indicated in Fig. 1, the histopathological analysis indicated a normal lung microstructure in uninfected animals, which was consistent with well-defined alveoli and alveolar sacs, thin

alveolar septa with low interstitial cellularity. All *S. mansoni*-infected mice exhibited interstitial retention of parasite eggs and marked granulomatous inflammation, which was associated with intense inflammatory infiltrate, lung granulomas with variable size, septal thickening and diffuse alveolar collapse. Animals in the group ShD2 presented larger granulomas predominantly in the productive stage. Conversely, smaller granulomas with involutive characteristics were mainly identified in the ShP group. Furthermore, EPO levels indicated intense eosinophil infiltration into the lung tissue of all infected animals compared to control mice ($p < 0.05$). EPO levels were respectively increased and reduced in the groups ShD2 and ShP ($p < 0.05$) compared to the groups Sh and ShD1, which exhibited similar results ($p > 0.05$) (Fig. 1).

Corroborating the histopathological findings, the morphometric results indicated that granuloma number and volume were higher in ShD2 animals ($p < 0.05$) and markedly reduced in the group ShP ($p < 0.05$) compared to Sh and ShD1 animals, which presented similar granuloma number and size ($p > 0.05$). The proportion of productive granuloma was similarly higher in the groups Sh and ShD1 compared to ShP animals ($p > 0.05$). Conversely, the distribution of involutive granulomas was significantly reduced in ShD2 animals ($p < 0.05$) and significantly increased in ShP mice ($p < 0.05$) compared to the groups Sh and ShD1. Granuloma size was coherent with lung accumulation of inflammatory cells, which was higher in ShD2 ($p < 0.05$) and reduced in ShP ($p < 0.05$) animals compared to the other infected groups (Fig. 2).

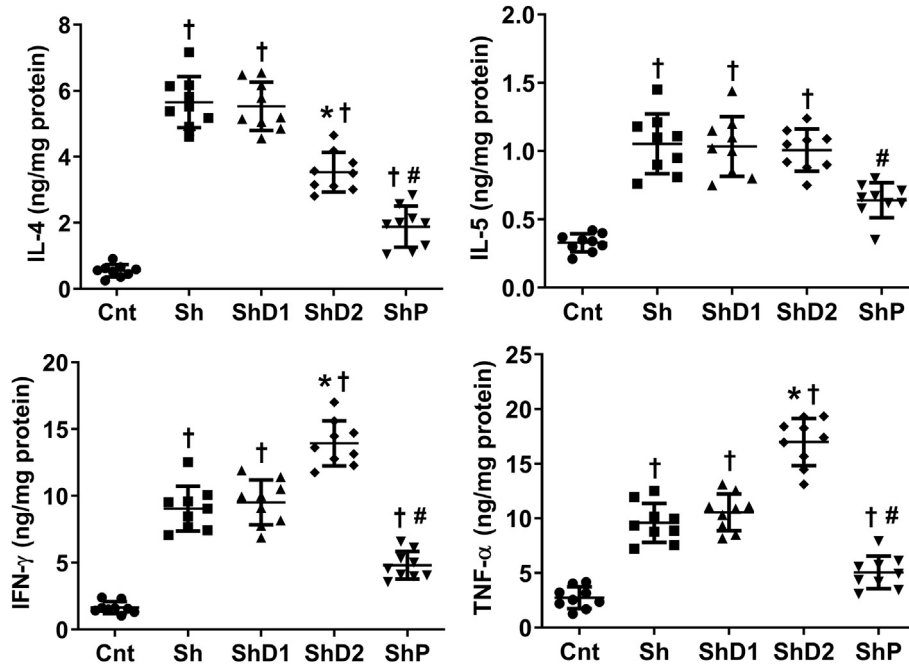


Fig. 3 Cytokine lung levels in control uninfected and *Schistosoma mansoni*-infected mice untreated and treated with doxycycline hyclate. Groups: Cnt: control uninfected untreated, Sh: infected with *S. mansoni*, ShD1: infected treated with doxycycline hyclate (5 mg/kg), ShD2: infected treated with doxycycline hyclate (50 mg/kg), ShP: infected treated with praziquantel (Pzt, 200 mg/kg). Data are expressed as mean and standard deviation. The points denote cytokine level obtained for each animal in all groups. The symbols in each group indicate statistical difference ($p \leq 0.05$), compared to † Cnt, * Sh and ShD1, # Sh, ShD1 and ShD2.

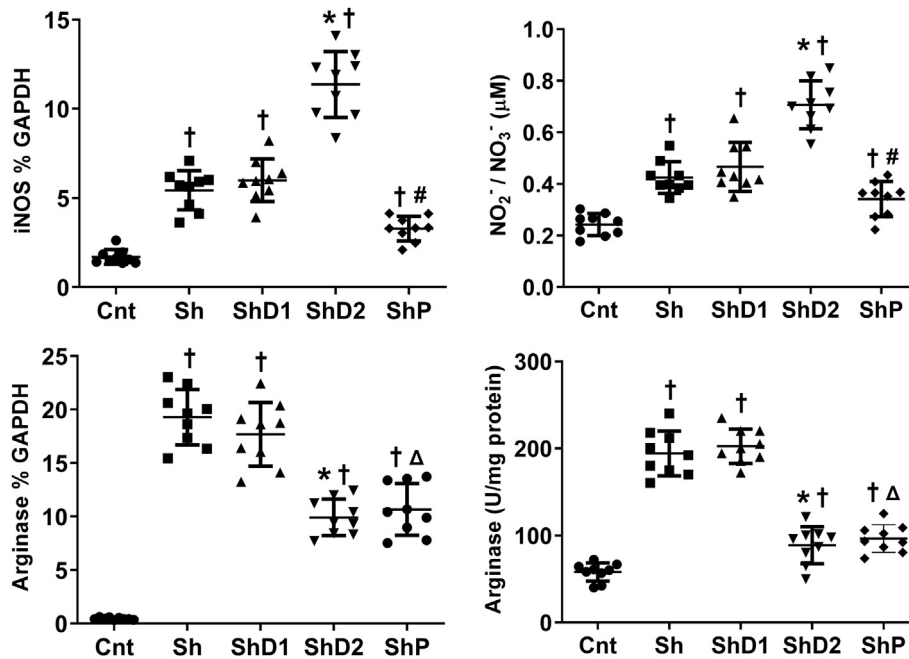


Fig. 4 Arginase and inducible nitric oxide synthase (iNOS), nitrite/nitrate (NO₂⁻/NO₃⁻) levels and arginase activity in lung samples from control uninfected and *Schistosoma mansoni*-infected mice untreated and treated with doxycycline hyclate. Groups: Cnt: control uninfected untreated, Sh: infected with *S. mansoni*, ShD1: infected treated with doxycycline hyclate (5 mg/kg), ShD2: infected treated with doxycycline hyclate (50 mg/kg), ShP: infected treated with praziquantel (Pzt, 200 mg/kg). Data are expressed as mean and standard deviation. The points denote cytokine level obtained for each animal in all groups. The symbols in each group indicate statistical difference ($p \leq 0.05$), compared to † Cnt, * Sh and ShD1, # Sh, ShD1 and ShD2, Δ Sh and ShD1.

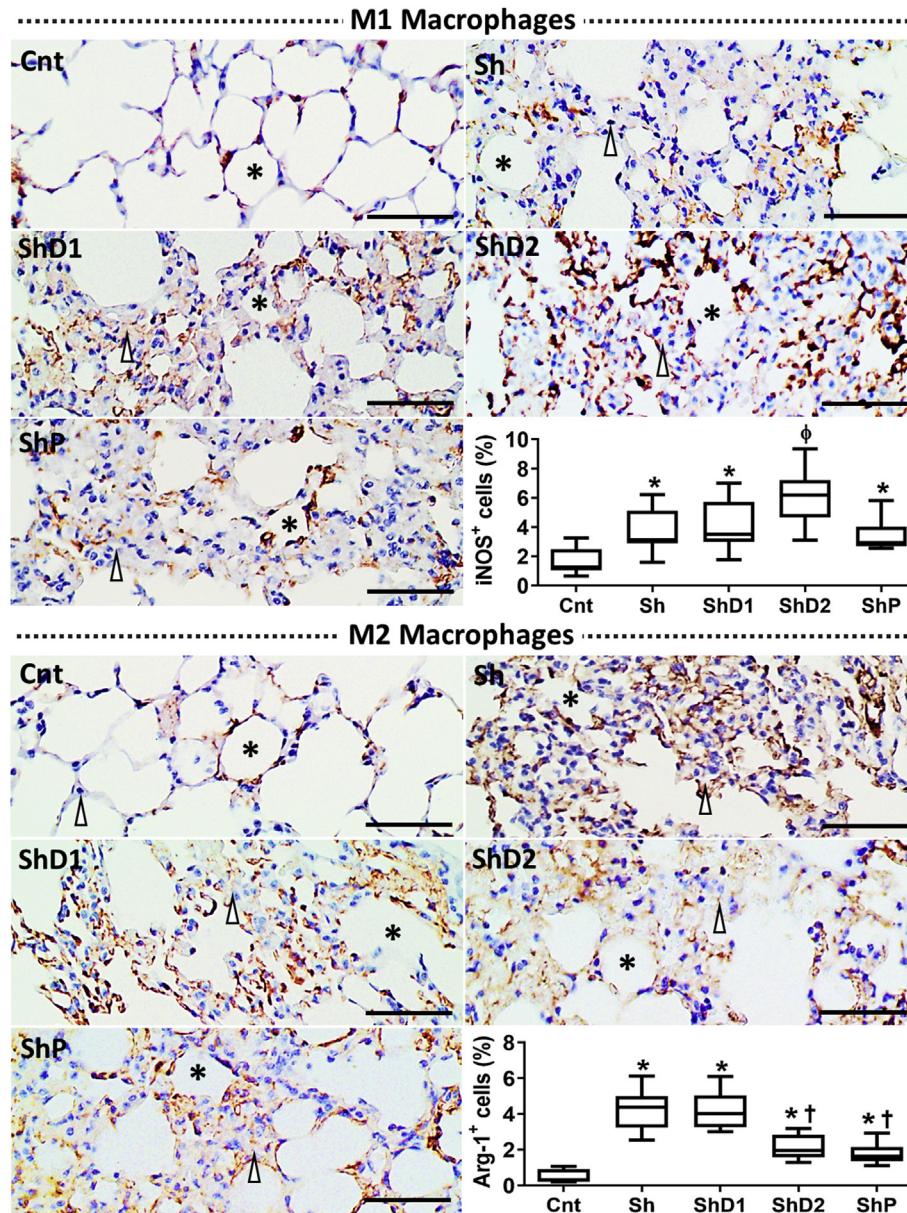


Fig. 5 Representative photomicrographs of the lungs of control uninfected and *Schistosoma mansoni*-infected mice untreated and treated with doxycycline hyclate submitted to immunohistochemistry for M1 (iNOS⁺ cells) and M2 (Arginase-1⁺ cells [Arg-1⁺]) macrophages (Bright field microscopy, scale bar = 60 μm). Macrophages are marked in brown in the histological images (Asterisk = alveoli, arrowhead = alveolar septum.) The relative distribution of M1 and M2 macrophages in each group is indicated in the graphics as median and interquartile range (statistical difference [$p < 0.05$] compared to *Cnt, †Sh and ShD1, ^φCnt, Sh, ShD1, and ShP). Groups: Cnt: control uninfected untreated, Sh: infected with *S. mansoni*, ShD1: infected treated with doxycycline hyclate (5 mg/kg), ShD2: infected treated with doxycycline hyclate (50 mg/kg), ShP: infected treated with praziquantel (Pzt, 200 mg/kg).

As indicated in Fig. 3, uninfected animals exhibited lower IL-4, IL-5, IFN- γ and TNF- α lung levels compared to the other groups ($p < 0.05$). IFN- γ and TNF- α levels were increased in ShD2 animals ($p < 0.05$) and reduced in ShP mice ($p < 0.05$) compared to the groups Sh and ShD1, which exhibited similar levels ($p > 0.05$) of all cytokines analyzed. IL-4 levels were higher in Sh and ShD1 animals compared to the other groups ($p < 0.05$). This cytokine was higher in the group ShD2

compared to ShP animals ($p < 0.05$). IL-5 was downregulated in ShP animals ($p < 0.05$) compared to the groups Sh, ShD1 and ShD2, which exhibited similar levels among them ($p > 0.05$).

Quantitative real-time PCR (Fig. 4) indicated increased iNOS and arginase gene expression, as well as NO levels and arginase activity in all infected groups compared to control animals ($p > 0.05$). iNOS gene expression and NO levels were upregulated in ShD2 animals compared to the other infected

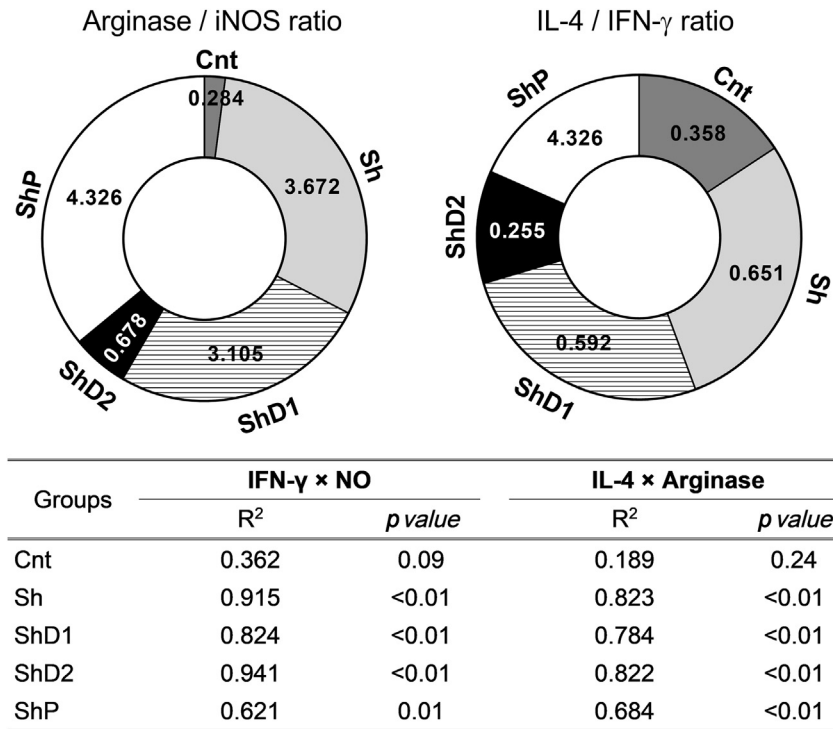


Fig. 6 Ratio between arginase/inducible nitric oxide synthase (iNOS) gene expression and between interleukin-4 (IL-4)/interferon gamma (IFN-γ) lung levels (top donut charts), and coefficient of determination (R²) between IFN-γ vs. nitric oxide (NO) levels and between IL-4 levels vs. arginase activity (bottom table). Groups: Cnt: control uninfected untreated, Sh: infected with *S. mansoni*, ShD1: infected treated with doxycycline hyclate (5 mg/kg), ShD2: infected treated with doxycycline hyclate (50 mg/kg), ShP: infected treated with praziquantel (Pzt, 200 mg/kg).

groups ($p < 0.05$). Arginase gene expression and arginase activity was similarly reduced in the groups ShD2 and ShP compared to Sh and ShD1 animals ($p < 0.05$).

From immunohistochemistry, M1 macrophages were identified with a diffuse distribution in the lungs of both uninfected and *S. mansoni*-infected animals. The immunostaining indicated a higher influx of M1 macrophages was observed in all infected animals compared to uninfected mice. An intense and diffuse immunohistochemical pattern of M1 macrophages was observed in the lungs of ShD2 animals. The qualitative observation was confirmed from image segmentation, which revealed that the histological area occupied by

M1 macrophages was higher in the groups ShD2 ($p > 0.05$) compared to the other groups (Fig. 5). A similarly greater accumulation of M2 macrophages was observed in Sh and ShD1 animals compared to the other groups ($p < 0.05$). This parameter was similar in ShD2 and ShP mice ($p > 0.05$), but higher compared to Cnt animals ($p < 0.05$).

As indicators of the balance between Th2 and Th1 immunological response, the ratio obtained for arginase/iNOS gene expression and IL-4/IFN-γ lung levels were significantly reduced in ShD2 animals compared to the other infected groups ($p < 0.05$). In addition, linear regression analysis indicated a direct and significant determination coefficient

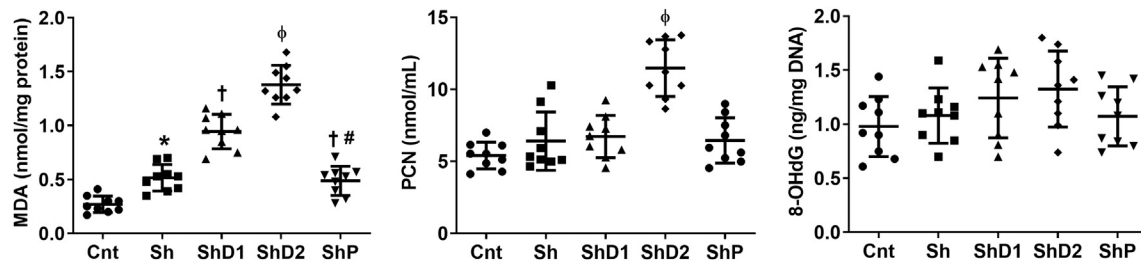


Fig. 7 Malondialdehyde (MDA), protein carbonyl (PCN) and 8-hydroxy-2'-deoxyguanosine (8-OHdG) levels in lung samples from control uninfected and *Schistosoma mansoni*-infected mice untreated and treated with doxycycline hyclate. Groups: Cnt: control uninfected untreated, Sh: infected with *S. mansoni*, ShD1: infected treated with doxycycline hyclate (5 mg/kg), ShD2: infected treated with doxycycline hyclate (50 mg/kg), ShP: infected treated with praziquantel (Pzt, 200 mg/kg). Data are expressed as mean and standard deviation. The points denote the levels of all oxidative markers for each animal in and groups. The symbols in each group indicate statistical difference ($p \leq 0.05$), compared to * Cnt, † Cnt and Sh, ‡ Cnt, Sh, ShD1 and ShP, § ShD1, # ShD1.

between IFN- γ and NO levels as well as between IL-4 levels and arginase activity in all infected groups. The higher determination coefficient was obtained between IFN- γ and NO levels in the group ShD2 (Fig. 6).

The biochemical analysis of lipid, protein and DNA oxidation (Fig. 7) indicated increased MDA lung levels in all infected groups, especially in ShD2 animals compared to the other groups ($p < 0.05$). This parameter was similar in Sh and ShP animals ($p > 0.05$), but reduced compared to ShD1 mice ($p < 0.05$). Higher PCN levels ($p < 0.05$) were observed in ShD2 animals compared to the other groups, which exhibited similar results ($p > 0.05$). 8-OHdG lung levels were similar in all groups ($p > 0.05$).

Discussion

The present study investigated the impact of Dox on Th1/Th2 effectors, M1 and M2 macrophages polarization, molecular oxidation and lung granulomatous inflammation in *S. mansoni*-infected mice. Our findings reinforced the evidence that *S. mansoni* infection upregulates Th2 effectors, stimulating intense IL-4 production and influx of M2-polarized macrophages. As expected, the reference drug Pzt exerted a protective effect by reducing Th1 and Th2 cytokine levels, lung inflammatory infiltrate, lipid peroxidation, the number and size of pulmonary granulomas, as well as accelerating granulomatous involution. Interestingly, the higher dose of Dox exerted an opposite immunomodulatory effect, subverting Th1/Th2 balance by upregulating Th1 cytokines, iNOS gene expression and NO production in detriment of Th2 cytokines, arginase gene expression and activity in infected mice. These effects were consistent with an increased leucocytes influx, reduced M2 and increased M1 macrophages accumulation, marked lipid and protein oxidation and extensive microstructural lung damage, indicating that Th1/Th2 imbalance and prooxidant events are potentially related to a more severe and less effective pulmonary inflammation in *S. mansoni*-infected and Dox-treated mice.

Extensive subversion of lung microstructure was observed in all groups infected by *S. mansoni*. In addition, intense granulomatous reaction and eosinophil infiltrate (indicated by EPO levels) were observed in untreated mice and especially in animals receiving the higher dose of Dox. Thus, the increased number of granulomas in Dox-treated mice indicated that this drug was ineffective to attenuate the infection as reported in different parasitic diseases such as malaria [12] and filariasis [14]. From the microstructural analysis, the intense cellularity in granulomas sheath corroborates that Dox potentiated leucocytes influx, especially macrophages and eosinophils, a finding closely correlated to the higher granulomas size and extensive alveolar collapse [15,37] compared to the other groups. Interestingly, the higher dose of Dox increased the distribution of productive granulomas, indicating a more active inflammatory process potentially related to the intense retention of parasite eggs in lung parenchyma [38]. Thus, Dox's inability to compromise the reproductive viability of *S. mansoni* ensures continuous deposition of parasite eggs in the

lung parenchyma, reinforcing the antigenic stimulation that drives the constant organization of new productive granulomas [2]. Conversely, the reduced number of predominantly involutive granulomas in Pzt-treated mice reinforces the schistosomicidal potential this drug. Thus, the effective parasites death by Pzt is consistent with reduced oviposition and eggs accumulation in lung parenchyma, as well as a consequent downregulation of proinflammatory stimuli, allowing the regression/reabsorption of old granulomas structured from eggs accumulated before Pzt treatment [15,18].

Within limits regulated by an adequate Th2 response, the granulomatous reaction is considered beneficial to the host. In this sense, granulomas imprison *S. mansoni* eggs, inhibiting immune hyperstimulation and tissue damage secondary to an exacerbated inflammatory process [6]. However, our findings indicated that Dox acted as a pharmacological risk factor, whose worsening of microstructural lung injury was potentially associated to the upregulation of molecular and cellular Th1 effectors and oxidative stress, which are known to increase the host's susceptibility to *S. mansoni* infection [10,11]. These proposition is reinforced by the increased IFN- γ , TNF- α , MDA and PCN lung levels, as well as reduced IL-4 production in animals receiving the highest dose of Dox. IL-4 is a cytokine typically secreted by Th2 cells, playing a central role in triggering a protective immune response against *S. mansoni*. This cytokine is highly expressed in chronic schistosomiasis and is required to orchestrate effective granulomatous reactions [39]. Curiously, a previous study reported an opposite IL-4 response in the liver from *S. mansoni*-infected mice treated with Dox [2]. Although a potential organ-dependent response is still poorly understood for this model of schistosomiasis, such divergence may be related to the variable parasite load at ectopic sites (i.e., eggs retention in the lungs) [40,41] and doxycycline biodistribution [42] in the lung and liver. As *S. mansoni* eggs are predominantly retained in the portal-caval venous blood channels [40], a higher antigenic load can amplify the immune stimulation and Th2 polarization in the liver, as supported by a more prominent IL-4 response in this organ [2]. Conversely, a reduced Dox accumulation [42] associated with a limited eggs retention in the lungs could attenuate the inflammatory stimulus for Th2 polarization, determining a reduced IL-4 production. Thus, the Th1 phenotype can more easily develop in the lungs as a counter-regulatory mechanism in order to achieve an immunological balance between these two response profiles, a proposition that requires further examination from comparative studies involving both organs.

Like IL-4, IL-5 is a Th2 cytokine often upregulated in schistosomiasis [43,44]. In addition to Th2 cells, innate effectors such as mast cells and eosinophils also secrete IL-5, whose initial production stimulates IL-4 biosynthesis and also plays an important role in recruiting cells (ie eosinophils) into parasitized organs in schistosomiasis [43,44]. In the present study, IL-5, lung inflammatory infiltrate and EPO levels were downregulated only in Pzt-treated mice, reinforcing the efficiency of the reference antiparasitic chemotherapy. As IL-4 but not IL-5, EPO levels and inflammatory infiltrate were attenuated in animals receiving the highest dose of Dx, our

findings suggest that this drug exerts a differential modulation on Th2 cytokines and leucocytes recruitment, an aspect that deserves to be elucidated in further studies. In this sense, high IL-5 levels seem to be potentially related to the intense eosinophils recruitment [43,44], a proposition reinforced by increased EPO lung levels in these animals, which was observed even with IL-4 downregulation. Conversely, IFN- γ and TNF- α are classical Th1 cytokines that stimulates intense leucocytes recruitment and marked activation of immunomediated oxidative and nitrosative mechanisms associated to tissue damage [6,11,15]. The involvement of IFN- γ , TNF- α , IL-4 and IL-5 in *S. mansoni*-induced granulomatous inflammation is corroborated by the reduced levels of all cytokines in Pzt-treated mice. Accordingly, an effective parasitic control by Pzt is aligned with the inhibition of the reproductive viability in *S. mansoni* (oviposition), representing realistic outcomes potentially linked to the marked attenuation of the immune response and granulomatous reaction in infected animals [45].

An attenuated Th2 response associated to the reciprocal Th1 and prooxidant reinforcement are corroborated by the downregulation in arginase expression and activity [46], as well as upregulation of iNOS expression and NO production [47] in animals treated with the highest dose of Dox. Considering that iNOS expression and NO production are typical effectors of M1 macrophages, while arginase pathway is essentially activated in M2 macrophages [48], our immunohistochemical findings were also consistent with an attenuated Th2 response in Dox-treated mice. Thus, the higher NO, MDA and PCN biosynthesis are also aligned with the severe lung microstructural damage (i.e., septal thickening and alveolar collapse) in Dox-treated animals, since reactive tissue damage is often associated to molecular and cellular Th1 effectors in parasitic diseases [49]. Cellular polarization dynamics is a highly regulated event, which is essentially involved in the modulation of host's susceptibility or resistance to different parasites [9,48]. Thus, variables combinations of Th1 and Th2 cytokines are determinants of macrophage polarization, with special relevance for IL-4 for the differentiation of M2 cells in chronic schistosomiasis [48,50]. Interestingly, the Th1 response is prevalent in acute schistosomiasis, which precedes *S. mansoni* oviposition. However, it is replaced by a Th2 response when the host is unable to eradicate persistent infection, but it should limit tissue damage and host mortality [9,51]. In this sense, IL-4-directed M2 activity is mainly associated to granuloma organization and tissue repair in a Th2-dominant response, which involves macrophages organization in highly cohesive concentric epithelioid arrangements and intense collagenogenesis to trap *S. mansoni* eggs and prevent hyperimmune activation [38,48]. Interestingly, granulomatous reaction was attenuated by Pzt. However, Pzt-treated mice exhibited increased distribution of M2 macrophages compared to uninfected animals, indicating that a persistent macrophage polarization accompanies the involutive remodeling of schistosomal granulomas in Pzt-treated mice, events potentially related to a Th1/Th2 rebalancing that requires further investigation.

Considering iNOS and arginase expression and NO production, as well as M1 and M2 macrophages distribution, our

findings reinforce the evidence that Th1 and Th2 are antagonist responses [48]. In this perspective, reduced M2 cells was consistent with the reduced arginase expression and activity in animals treated with the highest dose of Dox. Arginase hydrolyzes L-arginine in urea and L-ornithine, the latter being required for polyamines and proline biosynthesis, cell division and collagenogenesis [44,46]. Thus, arginase suppression can attenuates central events closely correlated to efficient granulomatous response in schistosomiasis [48,52]. Although the Th2 response is predominant in chronic schistosomiasis, the Th1 phenotype is not abolished [38]. Thus, our findings of IFN- γ , TNF- α , NO and M1 macrophages reinforce the evidence that Th1 activation acts as a counter-regulatory mechanism, which adjusts the intensity of the immune response in *S. mansoni*-infected untreated animals [9,53]. The balance between Th1 and Th2 effectors was clearly observed from the relationship between the classic markers of these polarized immunological phenotypes. In this sense, animals treated with the highest dose of Dox exhibited a marked reduction in arginase/iNOS and IL-4/IFN- γ ratio, reinforcing the evidence of an attenuated Th2 response. From this mechanism, Th2 subversion was potentially related to more severe lung inflammation, which was mainly expressed by excessive leucocytes recruitment with M1 macrophages accumulation, predominance of productive granulomas, and extensive alveolar collapse in Dox-treated mice. Except for control mice, all infected animals also showed a positive and significant correlation between IFN- γ and NO lung levels, as well as between IL-4 and arginase activity. These findings reinforce the dependence relationship between classic Th1 and Th2 effectors in schistosomiasis, especially considering that IFN- γ and IL-4 are the most prominent stimuli for the respective activation of the iNOS and arginase pathways [9]. Thus, the validity of these effectors as specific indicators of the Th1 and Th2 phenotypes are reinforced in our murine model of *S. mansoni* infection, especially considering that IFN- γ /NO and IL-4/arginase correlations were maintained in Dox- and Pzt-treated animals.

Conclusions

Taken together, our findings provide the evidence that Dox acts as a pharmacological risk factor in schistosomiasis by aggravating lung granulomatous inflammation in a dose-dependent way. While *S. mansoni* infection upregulates Th2 effectors, stimulating intense IL-4 production and M2 macrophages recruitment, Dox attenuated this response by subverting Th1/Th2 balance. Thus, Dox reinforces Th1 cytokines, M1 macrophages accumulation, iNOS gene expression and NO production in detriment of arginase gene expression and activity, Th2 cytokines production, and M2 macrophages polarization in *S. mansoni*-infected mice. These effects occurred concurrently with an increased eosinophil recruitment, intense inflammatory infiltrate poor in M2 cells, marked lipid and protein oxidation and extensive microstructural lung damage, indicating that a Th1/Th2 imbalance and prooxidant events are potentially related to a more severe and less effective lung inflammation in *S. mansoni*-infected and Dox-treated mice.

Conflicts of interest

None.

Acknowledgements

This work was supported by the Brazilian agencies: Fundação do Amparo à Pesquisa do Estado de Minas Gerais (FAPEMIG, processes PPM-00077-18 and PPM-00687-17) and Conselho Nacional de Desenvolvimento Científico e Tecnológico (CNPq, processes 310331/2020-0, 423594/2018-4, 408503/2018-1 and 311105/2020-3). This study was financed in part by the Coordenação de Aperfeiçoamento de Pessoal de Nível Superior - Brasil (CAPES) – Finance Code 001.

REFERENCES

- [1] McManus DP, Dunne DW, Sacko M, Utzinger J, Vennervald BJ, Zhou XN. Schistosomiasis. *Nat Rev Dis Prim* 2018;4:13.
- [2] Dias MV, Castro AP, Campos CC, Souza-Silva TG, Gonçalves RV, Souza RLM, et al. Doxycycline hyclate: a schistosomicidal agent in vitro with immunomodulatory potential on granulomatous inflammation in vivo. *Int Immunopharm* 2019;70:324–37.
- [3] Melo EV, Costa Wd, Conceição MJ, Coura JR. A comparative cross-sectional study on the prevalence and morbidity of schistosomiasis in a community in northeastern Brazil (1979–2010). *Mem Inst Oswaldo Cruz* 2014;109:340–4.
- [4] Souza COS, Gardinassi LG, Rodrigues V, Faccioli LH. Monocyte and macrophage-mediated pathology and protective immunity during schistosomiasis. *Front Microbiol* 2020;11:1973.
- [5] Colley DG, Bustinduy AL, Secor WE, King CH. Human schistosomiasis. *Lancet* 2014;383:2253–64.
- [6] Llanwarne F, Helmby H. Granuloma formation and tissue pathology in *Schistosoma japonicum* versus *Schistosoma mansoni* infections. *Parasite Immunol* 2021;43:e12778.
- [7] Lambertucci JR, Falcheto EB, Santos VA. Dilated paraumbilical vein in hepatosplenic schistosomiasis is associated with pulmonary hypertension. *Rev Soc Bras Med Trop* 2013;46:797.
- [8] Herbert DR, Hölscher C, Mohrs M, Arendse B, Schwegmann A, Radwanska M, et al. Alternative macrophage activation is essential for survival during schistosomiasis and downmodulates T helper 1 responses and immunopathology. *Immunity* 2004;20:623–35.
- [9] Barron L, Wynn TA. Macrophage activation governs schistosomiasis-induced inflammation and fibrosis. *Eur J Immunol* 2011;41:2509–14.
- [10] La Flamme AC, Patton EA, Bauman B, Pearce EJ. IL-4 plays a crucial role in regulating oxidative damage in the liver during schistosomiasis. *J Immunol* 2001;166:1903–11.
- [11] Rodrigues JPF, Caldas IS, Gonçalves RV, Almeida LA, Souza RLM, Novaes RD. *S. mansoni*-*T. cruzi* co-infection modulates arginase-1/iNOS expression, liver and heart disease in mice. *Nitric Oxide* 2017;66:43–52.
- [12] Rajendran V, Singh C, Ghosh PC. Improved efficacy of doxycycline in liposomes against *Plasmodium falciparum* in culture and *Plasmodium berghei* infection in mice. *Can J Physiol Pharmacol* 2018;96:1145–52.
- [13] De Paula Costa G, Lopes LR, da Silva MC, Horta AL, Pontes WM, Milanezi CM, et al. Doxycycline and benznidazole reduce the profile of Th1, Th2, and Th17 chemokines and chemokine receptors in cardiac tissue from chronic *Trypanosoma cruzi*-infected dogs. *Mediat Inflamm* 2016;2016:3694714.
- [14] Hoerauf A, Mand S, Fischer K, Kruppa T, Marfo-Debrekyei Y, Debrah AY, et al. Doxycycline as a novel strategy against bancroftian filariasis-depletion of *Wolbachia* endosymbionts from *Wuchereria bancrofti* and stop of microfilaria production. *Med Microbiol Immunol* 2003;192:211–6.
- [15] Santos MP, Gonçalves-Santos E, Gonçalves RV, Santos EC, Campos CC, Bastos DSS, et al. Doxycycline aggravates granulomatous inflammation and lung microstructural remodeling induced by *Schistosoma mansoni* infection. *Int Immunopharm* 2021;94:107462.
- [16] Rocha Pereira AE, Rodrigues MÂ, Novaes RD, Caldas IS, Martins Souza RL, Costa Pereira AA. Lipopolysaccharide-induced acute lung injury in mice chronically infected by *Schistosoma mansoni*. *Exp Parasitol* 2017;178:21–9.
- [17] de Araújo MP, Burger E, Dias Novaes R, Ami Akatuti A, Rodrigues MÂ, Mendes ACSC, et al. Impact of *Paracoccidioides brasiliensis* coinfection on the evolution of *Schistosoma mansoni*-induced granulomatous liver injury in mice. *BioMed Res Int* 2019;2019:8319465.
- [18] Araújo N, Mattos AC, Sarvel AK, Coelho PM, Katz N. Oxamniquine, praziquantel and lovastatin association in the experimental *Schistosomiasis mansoni*. *Mem Inst Oswaldo Cruz* 2008;103:450–4.
- [19] Reis MÂ, Novaes RD, Baggio SR, Viana ALM, Salles BCC, Duarte SMDS, et al. Hepatoprotective and antioxidant activities of oil from baru almonds (*Dipteryx alata* Vog.) in a preclinical model of lipotoxicity and dyslipidemia. *Evid Based Complement Alternat Med* 2018;2018:8376081.
- [20] Lacerda AC, Rodrigues-Machado Mda G, Mendes PL, Novaes RD, Carvalho GM, Zin WA, et al. Paraquat (PQ)-induced pulmonary fibrosis increases exercise metabolic cost, reducing aerobic performance in rats. *J Toxicol Sci* 2009;34:671–9.
- [21] Cardoso LM, Novaes RD, de Castro CA, Novello AA, Gonçalves RV, Ricci-Silva ME, et al. Chemical composition, characterization of anthocyanins and antioxidant potential of *Euterpe edulis* fruits: applicability on genetic dyslipidemia and hepatic steatosis in mice. *Nutr Hosp* 2015;32:702–9.
- [22] Novaes RD, Gonçalves RV, Cupertino MC, Marques DC, Rosa DD, Peluzio Mdo C, et al. Bark extract of *Bathysa cuspidata* attenuates extra-pulmonary acute lung injury induced by paraquat and reduces mortality in rats. *Int J Exp Pathol* 2012;93:225–33.
- [23] Novaes RD, Gonçalves RV, Penitente AR, Bozi LH, Neves CA, Maldonado IR, et al. Modulation of inflammatory and oxidative status by exercise attenuates cardiac morphofunctional remodeling in experimental Chagas cardiomyopathy. *Life Sci* 2016;152:210–9.
- [24] Gonçalves RV, Santos JDB, Silva NS, Guillocheau E, Silva RE, Souza-Silva TG, et al. Trans-fatty acids aggravate anabolic steroid-induced metabolic disturbances and differential gene expression in muscle, pancreas and adipose tissue. *Life Sci* 2019;232:116603.
- [25] Rosa CP, Pereira JA, Cristina de Melo Santos N, Brancaglioni GA, Silva EN, Tagliati CA, et al. Vancomycin-induced gut dysbiosis during *Pseudomonas aeruginosa* pulmonary infection in a mice model. *J Leukoc Biol* 2020;107:95–104.
- [26] Jo J, Choi MY, Koh DS. Size distribution of mouse Langerhans islets. *Biophys J* 2007;93:2655–66.

- [27] Khoury P, Makiya M, Klion AD. Clinical and biological markers in hypereosinophilic syndromes. *Front Med (Lausanne)* 2017;4:240.
- [28] Bradford MM. A rapid and sensitive method for the quantitation of microgram quantities of protein utilizing the principle of protein-dye binding. *Anal Biochem* 1976;72:248–54.
- [29] Santos EC, Novaes RD, Cupertino MC, Bastos DS, Klein RC, Silva EA, et al. Concomitant benznidazole and suramin chemotherapy in mice infected with a virulent strain of *Trypanosoma cruzi*. *Antimicrob Agents Chemother* 2015;59:5999–6006.
- [30] Felizardo AA, Caldas IS, Mendonça AAS, Gonçalves RV, Tana FL, Almeida LA, et al. Impact of *Trypanosoma cruzi* infection on nitric oxide synthase and arginase expression and activity in young and elderly mice. *Free Radic Biol Med* 2018;129:227–36.
- [31] Tsikas D. Analysis of nitrite and nitrate in biological fluids by assays based on the Griess reaction: appraisal of the Griess reaction in the L-arginine/nitric oxide area of research. *J Chromatogr B Anal Technol Biomed Life Sci* 2007;15:51e70.
- [32] Novaes RD, Santos EC, Fialho MDCQ, Gonçalves WG, Sequetto PL, Talvani A, et al. Nonsteroidal anti-inflammatory is more effective than anti-oxidant therapy in counteracting oxidative/nitrosative stress and heart disease in *T. cruzi*-infected mice. *Parasitology* 2017;144:904–16.
- [33] Levine RL, Garland D, Oliver CN, Amici A, Climent I, Lenz AG, et al. Determination of carbonyl content in oxidatively modified proteins. *Methods Enzymol* 1990;186:464–78.
- [34] Venosa A, Malaviya R, Choi H, Gow AJ, Laskin JD, Laskin DL. Characterization of distinct macrophage subpopulations during nitrogen mustard-induced lung injury and fibrosis. *Am J Respir Cell Mol Biol* 2016;54:436–46.
- [35] Rószter T. Understanding the Mysterious M2 Macrophage through activation markers and effector mechanisms. *Mediat Inflamm* 2015;2015:816460.
- [36] Novaes RD, Cupertino MC, Sarandy MM, Souza A, Soares EA, Gonçalves RV. Time-dependent resolution of collagen deposition during skin repair in rats: a correlative morphological and biochemical study. *Microsc Microanal* 2015;21:1482–90.
- [37] Lichtenberg V. Host response to eggs of *S. mansoni*. I. Granuloma formation in the unsensitized laboratory mouse. *Am J Pathol* 1962;41:711–31.
- [38] Schwartz C, Fallon PG. *Schistosoma* "Eggs-Itting" the host: granuloma formation and egg excretion. *Front Immunol* 2018;9:2492.
- [39] Kumar R, Mickael C, Chabon J, Gebreab L, Rutebemberwa A, Garcia AR, et al. The causal role of IL-4 and IL-13 in *Schistosoma mansoni* pulmonary hypertension. *Am J Respir Crit Care Med* 2015;192:998–1008.
- [40] Faust EC. An inquiry into the ectopic lesions in schistosomiasis. *Am J Trop Med Hyg* 1948;28:175–99.
- [41] De Faria JL. Pulmonary arteriovenous fistulas and arterial distribution of eggs of *Schistosoma mansoni*. *Am J Trop Med Hyg* 1956;5:860–2.
- [42] İlem-Özdemir D, Asikoglu M, Ozkilic H, Yilmaz F, Hosgor-Limoncu M, Ayhan S. Tc-Doxycycline hyclate: a new radiolabeled antibiotic for bacterial infection imaging. *J Label Compd Radiopharm* 2014;57:36–41. 99m.
- [43] Sher A, Coffman RL, Hieny S, Scott P, Cheever AW. Interleukin 5 is required for the blood and tissue eosinophilia but not granuloma formation induced by infection with *Schistosoma mansoni*. *Proc Natl Acad Sci USA* 1990;87:61–5.
- [44] Sabin EA, Kopf MA, Pearce EJ. *Schistosoma mansoni* egg-induced early IL-4 production is dependent upon IL-5 and eosinophils. *J Exp Med* 1996;184:1871–8.
- [45] Vale N, Gouveia MJ, Rinaldi G, Brindley PJ, Gärtner F, Correia da Costa JM. Praziquantel for schistosomiasis: single-drug metabolism revisited, mode of action, and resistance. *Antimicrob Agents Chemother* 2017;61:e02582-16.
- [46] Stempin CC, Dulgerian LR, Garrido VV, Cerban FM. Arginase in parasitic infections: macrophage activation, immunosuppression, and intracellular signals. *J Biomed Biotechnol* 2010;2010:683485.
- [47] Angeles JMM, Mercado VJP, Rivera PT. Behind Enemy Lines: immunomodulatory armamentarium of the schistosome parasite. *Front Immunol* 2020;11:1018.
- [48] Hesse M, Modolell M, La Flamme AC, Schito M, Fuentes JM, Cheever AW, et al. Differential regulation of nitric oxide synthase-2 and arginase-1 by type 1/type 2 cytokines in vivo: granulomatous pathology is shaped by the pattern of L-arginine metabolism. *J Immunol* 2001;167:6533–44.
- [49] de Carvalho RVH, Zamboni DS. Inflammasome activation in response to intracellular protozoan parasites. *Trends Parasitol* 2020;36:459–72.
- [50] Wang N, Liang H, Zen K. Molecular mechanisms that influence the macrophage M1-M2 polarization balance. *Front Immunol* 2014;5:614.
- [51] Costain AH, MacDonald AS, Smits HH. Schistosome egg migration: mechanisms, pathogenesis and host immune responses. *Front Immunol* 2018;9:3042.
- [52] Pesce JT, Ramalingam TR, Mentink-Kane MM, Wilson MS, El Kasbi KC, Smith AM, et al. Arginase-1-expressing macrophages suppress Th2 cytokine-driven inflammation and fibrosis. *PLoS Pathog* 2009;5:e1000371.
- [53] Rani R, Jordan MB, Divanovic S, Herbert DR. IFN- γ -driven Ido production from macrophages protects IL-4R α -deficient mice against lethality during *Schistosoma mansoni* infection. *Am J Pathol* 2012;180:2001-8.